A Solid-State Regenerative Repeater for Guided Millimeter-Wave Communication Systems

By W. M. HUBBARD, J. E. GOELL, W. D. WARTERS, R. D. STANDLEY, G. D. MANDEVILLE, T. P. LEE, R. C. SHAW, and P. L. CLOUSER

(Manuscript received July 20, 1967)

Recent advances in solid-state device technology for generating millimeter waves as well as advances in component design for IF and baseband portions of repeaters have renewed interest in millimeter-wave guided-wave communication systems. This paper describes a 306 Mb/s, all solid-state repeater which has been built using a 1.3-GHz IF and a form of differentially-coherent phase modulation. A signal-to-noise ratio of 13.6 dB is required for an error probability of 10^{-9} (compared with a theoretical value of 13.0 dB for an ideal differentially-coherent phase-modulated system). Sufficient gain for 15-mile repeater spacings (using two-inch circular waveguide) has been obtained with an LSA diode, an IMPATT diode, and a varactor multiplier as the millimeter-wave power source.

I. INTRODUCTION

1.1 *Guided Millimeter-Wave Communication Systems*

High-speed, long-haul communication by means of millimeter waves transmitted in the circular-electric mode in a multimode circular waveguide was described by S. E. Miller[1] in 1954. Recent advances in solid-state devices for generating millimeter waves as well as advances in circuit design for the IF and baseband portions of the repeaters have renewed interest in such a system.

The purpose of this paper is to describe the design and performance of an experimental all solid-state millimeter-wave repeater which has recently been built and tested. It operates at a carrier frequency of 51.7 GHz and transmits binary PCM at a 306 Mb/s rate. The experimental repeater includes all of the active circuitry for one channel of

a complete repeater and contains channel filters representative of those needed to separate and combine the many channels of an actual system. It was built to demonstrate certain principles and no attempt is made here to describe or design a complete system. Certain system considerations are discussed in Section IV in order to give the reader some perspective concerning those factors which influenced the design of the repeater.

In section II, we discuss a modulation scheme which was conceived to satisfy the requirement imposed by the nature of the system. The circuitry used in the repeater is discussed in Section III. Particular emphasis is placed on those portions of the circuit which the authors feel represent a significant advance in the state of the art. The performance of the repeater is described in Section V. Finally, the conclusions which are to be drawn from the experimental performance of the repeater are summarized in Section VI.

For a given repeater gain and spacing the communication capacity of such a system is set by the attenuation characteristics of the waveguide. The system under consideration would use TE_{01} mode transmission in 2-inch helix or dielectric-lined circular waveguides.

The characteristics of these kinds of waveguides have been studied theoretically by H. E. Rowe and W. D. Warters,[2] S. P. Morgan and J. A. Young,[3] and H. G. Unger;[4] and studied experimentally by A. P. King and G. D. Mandeville[5] and W. H. Steier[6] for a straight waveguide. More recently a study of typical route loss has been undertaken by W. G. Nutt and others.[7] Their results, shown in Fig. 1 along with the results of the other measurements cited above, are used for the calculations in Section 4.1. From these measurements, one finds that

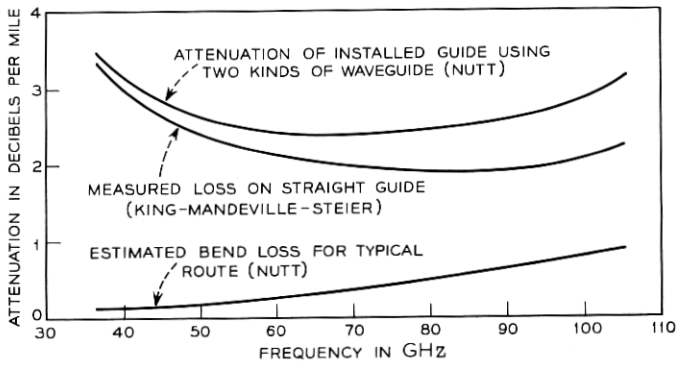

Fig. 1 — TE_{01}, mode attenuation characteristic of 2-inch circular waveguide.

the attenuation is less than 3 dB per mile over a band of frequencies extending from approximately 40 GHz to 100 GHz. This 60-GHz band of frequencies is considered the "usable bandwidth" of the waveguide. In Section IV, it is shown that approximately 200,000 two-way voice channels can be accommodated by the waveguide if 9 digit binary PCM transmission is used.

The purpose of this experiment was to demonstrate the feasibility of building repeaters for a millimeter-wave communication system. When this experiment was begun early in 1966, the band-splitting filters and the IF amplifiers had already been developed and no problems were expected in these areas—and in fact, none arose. Our initial efforts were concerned with building filters for dropping the individual channels and for injection of local oscillator power into the up- and down-converters, providing a source of millimeter-wave power, building up- and down-converters with attractive conversion loss, building FM deviators, and building baseband and timing recovery circuitry which would operate at the 306 Mb/s rate. Soon after this work began, the LSA (Limited Space-charge Accumulation) oscillator was developed by J. A. Copeland.[8] It provides what seems to be a suitable millimeter-wave power source. In addition, a 12.6-GHz IMPATT (IMPact Ionization Avalanche Transit Time) diode driving a quadrupler, provides a suitable power source. More recently, a 50.4-GHz IMPATT diode has been successfully tested as a millimeter-wave power source. The other components were developed during the course of the experiment. Thus, it has been demonstrated that such a system is within the present state of the art.

One significant component, a delay distortion equalizer, which will be required in an actual system, was not considered in this experiment. Several possible equalizers have been proposed in the past and while considerable study is still required before a choice can be made from among these alternatives, there do not seem to be any problems associated with equalization that would affect the feasibility of the system. A review of some work which has been done on equalization of delay distortion is presented briefly in Appendix A.

II. MODULATION

2.1 *Modulation Requirements*

It was felt that the modulation scheme used in this repeater should satisfy four important requirements. First, in order to make efficient

use of the limited power available from solid-state devices—especially at millimeter-wave frequencies—it is important to use a type of modulation which gives good noise immunity, that is, one which will provide an acceptable error-rate with relatively small signal-to-noise ratio.

Second, because the repeaters are to be regenerative, timing information must be provided at each repeater. While this can be accomplished in several ways, a very attractive way is to use a type of modulation which allows the repeater to extract timing directly from the signal regardless of message statistics. This eliminates the necessity of sending timing information on a separate channel or of including pulses into the bit stream to insure a timing signal even in the event the message causes a particularly unfavorable pulse pattern.

Third, since the system is to operate at very high bit rates, it is important that the modulation scheme be one which can be implemented with a minimum of circuitry.

Finally, the modulation scheme must not be excessive in its bandwidth requirement even though, due to the large bandwidth capability of the waveguide, one is willing to make a reasonable trade of bandwidth for noise immunity.

The optimum noise immunity (consideration 1) would be achieved with binary coherent phase-shift-keyed modulation.[9] However, this type of modulation requires that a reference phase be provided at each repeater. The need for a reference signal is eliminated by using a differentially-coherent signal at a cost of less than 0.5 dB in noise immunity at acceptable error rates (the order of one error in 10^9 bits), as can be calculated from the equations in a review paper by J. G. Lawton.[10]

2.2 *Description of FM-DCPSK*

A modulation scheme which we have designated FM-DCPSK (Frequency-Modulated Differentially-Coherent Phase-Shift-Keyed) modulation was conceived as a reasonable compromise among the four considerations. FM-DCPSK is a hybrid of frequency modulation and differentially-coherent phase-shift-keyed modulation. The signal has constant amplitude and is angle modulated in such a way that the information is carried in the relative phase, i.e., the phase shift between adjacent sampling instants. Optimum noise immunity occurs when the two possible signal states in a given time slot differ in phase by π. This can be achieved by shifting the phase by an amount $+\pi/2$ or

$-\pi/2$ between successive time slots (the choice of the sign depending on the message). A signal-space diagram is shown in Fig. 2. Fig. 3 shows the variation of phase and frequency resulting from modulation with the binary train indicated at the top of the figure. It will become apparent when we discuss repeater circuits in Section III that the simplicity consideration is satisfied by the FM-DCPSK signal.

Modulation from polar binary baseband to carrier IF is performed directly with an FM deviator. No flip-flop or other binary to differential-binary translator is required because of the differential relationship between frequency and phase. The deviator linearity is unimportant since only the area under the frequency-versus-time curve is important. The constant-amplitude continuous-phase nature of the signal allows phase-locked oscillators to be used for gain and limiting.

Because there is a phase change (hence, a frequency swing) in each time slot, regardless of the signal statistics, timing information is available in the signal itself. This can be readily extracted by means of a frequency discriminator and a narrow bandpass filter as described in Section 3.9. Finally, the bandwidth which gives optimum results is found experimentally to be slightly larger than the bit rate, which is in agreement with theoretical calculations for frequency modulated systems by R. R. Anderson and J. Salz.[11]

III. CIRCUITRY FOR THE REPEATER

3.1 *Introduction*

The repeater circuit is shown in block diagram form in Fig. 4. Fig. 5 is a photograph of the repeater. This subsection will give a brief introductory discussion of the layout and operation of the repeater. Detailed discussion of the operation of various components is deferred to the following subsections.

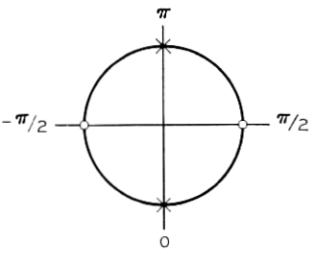

Fig. 2 — Signal space diagram for binary FM-DCPSK $\phi_n = 0$ or π for $n = n_0$, $n_0 + 2$, $n_0 + 4, \ldots\ldots, \phi_n = +\pi/2$ or $-\pi/2$ for $n = n_0 + 1$, $n_0 + 3$, $n_0 + 5, \ldots\ldots$

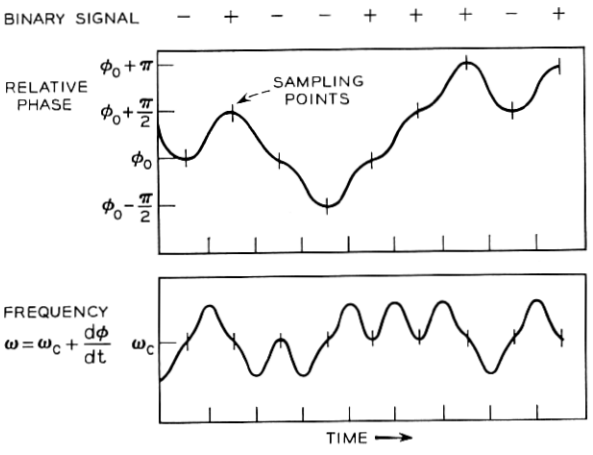

Fig. 3 — Phase and frequency variations of a FM-DCPSK signal.

The signal enters in the TE_{01} mode in 2-inch circular waveguide and first encounters a band-splitting filter which divides the 60-GHz band of the waveguide into two sub-bands. The signal in each of these sub-bands next encounters a channel-dropping filter which drops the individual channel for the individual repeater. In an actual system, several (perhaps as many as six) band-splitting filters would be used and a string of several (perhaps as many as 30) channel-dropping filters would follow each band-splitting filter. The first component which the individual signal encounters after the channel-dropping filter is a down-converter which translates the millimeter-wave signal frequency to the 1.3-GHz IF frequency of the repeater. The down-converter is followed by a low-noise transistor amplifier which provides approximately 52 dB of gain. This amplified signal is then used to lock an oscillator which serves as a limiter. The output of this limiter is amplified by a second transistor amplifier having 27 dB of gain. The next component is a combination differential-phase detector and timing recovery circuit. This component provides both a timing signal which consists of a sine wave at the bit frequency recovered from the transmitted signal and a baseband information signal whose polarity depends on the binary information transmitted. This polar baseband signal is then applied to a regenerator along with the timing signal and the regenerator makes a decision as to which of the binary states was transmitted in each time slot. The output of the regenerator drives an FM deviator which provides an

angle-modulated signal at IF. This signal is amplified by a third transistor IF amplifier and up-converted to the original millimeter-wave frequency. This millimeter-wave signal is now combined with the signals in other channels by means of a series of channel-adding filters and band-combining filters which are identical to the channel-dropping and band-splitting filters used at the input. The output is again in the TE_{01} mode in 2-inch circular waveguide.

3.2 *Band-Splitting Filters*

The band-splitting filters perform the function of splitting the 40-GHz to 100-GHz band into relatively wide sub-bands. The devices used for this purpose have been described in detail by Marcatili and Bisbee.[12] For completeness, their scheme will be reviewed briefly. Fig. 6 shows a constant resistance filter made up of two hybrids connected together by two identical high-pass filters.

Power entering port 1 is equally split by the hybrid H_1 with each

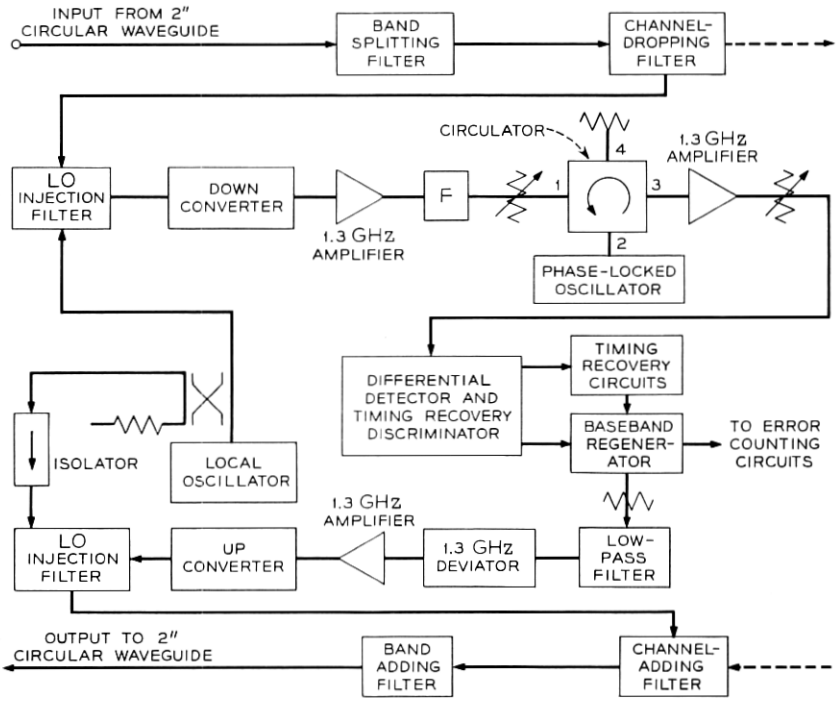

Fig. 4 — Repeater circuitry.

half propagating through equal line lengths toward the high-pass filters. Frequencies above the cutoff frequency of the high-pass filters pass through the filters unattenuated, are recombined in the second hybrid and emerge at port 4. Frequencies below the cutoff frequency of the high-pass filters are reflected back towards the first hybrid where they recombine and emerge at port 2. Marcatili and Bisbee realized this structure in low-loss TE_{01} circular electric mode components.

The hybrids developed consist of a right angle tee junction of two, 2-inch i.d. round waveguides with a thin sheet of dielectric material placed diagonally across the junction. The system can be analyzed on a quasi-optical basis with the result that proper selection of the dielectric material produces hybrid performance.

The high-pass filters used were TE_{01} mode guides with cutoff frequency equal to the splitting frequency. They were coupled to the 2-inch helix guides by means of helix waveguide tapers. Experimental results on a composite filter show that the maximum loss in either subband is 1.5 dB and that the transition region takes up only 160 MHz of the spectrum.

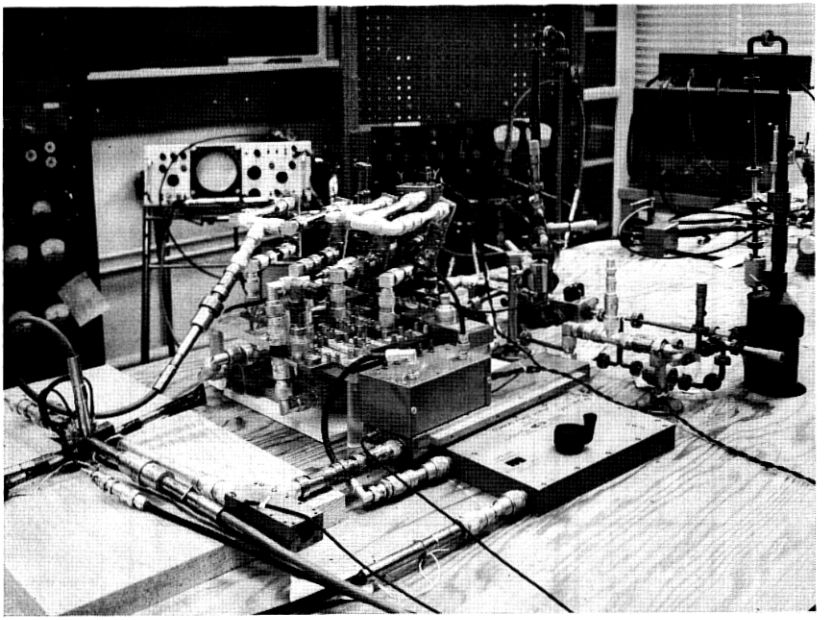

Fig. 5 — Experimental model of millimeter-wave repeater.

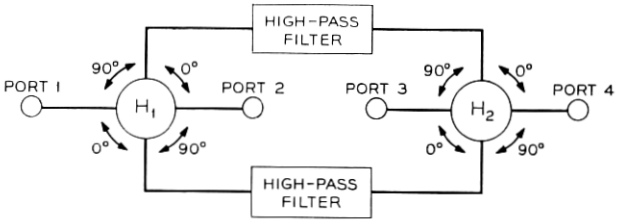

Fig. 6 — Band-splitting filter. H_1 and H_2 are hybrids (taken from Ref. 12).

3.3 *Channel-Dropping Filters*

The requirements for the channel-dropping filters are determined by such factors as tolerable insertion loss, intersymbol interference, and interchannel interference. Explicit analysis of intersymbol interference and inter-channel interference problems associated with the type modulation used is as yet incomplete. Hence, a procedure for optimizing channel to channel spacing is not available.

For the experimental repeater, attention was directed to two-pole, wideband channel-dropping filters because they afford a significant reduction in required channel spacing relative to that for single pole filters. A bandwidth of 1 GHz was chosen to prove the flexibility of the design procedure. The theory developed[13] employed narrow bandwidth approximations; thus, the design of filters having smaller bandwidth would be no problem. As stated in Section 2.2 an overall channel bandwidth slightly greater than the bit rate yields optimum error rate. Based on this fact, consideration of all of the band-limiting elements in a given channel indicates that channel-dropping filter bandwidths of less than twice the bit rate will be adequate.

Fig. 7 shows the physical structure and identifies the resonant elements of the channel-dropping filters. Ports 1 and 3 are the circular mode input and output ports, respectively. Port 2 is the dropped (or added) channel output (or input) port. The input and output guides are above cutoff for the TE_{01} mode and just below cutoff for the TE_{02} mode. The large guide sections are just above cutoff for the TE_{02} mode. The rectangular waveguide output is coupled to the mode-conversion resonator nearest the input by means of a wrapped resonator of rectangular cross section.

A qualitative description of the behavior of the structure is as follows. First, consider an individual rejection resonator. A signal incident in the TE_{01} mode is coupled to the TE_{02} mode by means of a symmetrical diameter discontinuity. Since the input and output

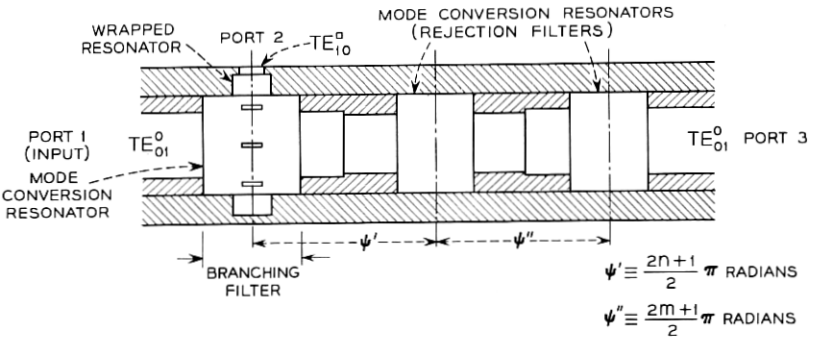

Fig. 7 — Cross section view of channel-dropping filter.

guides are below cutoff for the TE_{02} mode, the power in that mode is trapped in the large diameter region. Marcatili's analysis of the structure shows that at resonance the transverse mid-plane of the resonator is effectively a short circuit.[14] The center frequency and bandwidth are dependent on the length of the resonator and the ratio of the input guide diameter to the resonator diameter. The details of the relationship are given by Marcatili.[14]

In the structure of Fig. 7, the mid-planes of adjacent mode-conversion resonators are electrically separated by odd multiples of $\pi/2$ radians. Hence, at resonance, the rejection-resonator pair presents an open circuit at the mid-plane of the input mode-conversion resonator. All of the incident TE_{01} mode power appears at the rectangular waveguide output when the various coupling coefficients are properly chosen.

Further insight into the electrical behavior of the structure is obtained by considering the prototype network shown in Fig. 8. The prototype network consists of complimentary admittances connected in shunt. The elements of the network have been chosen to yield a two-pole, maximally flat insertion loss response between ports 1 and 2 while maintaining a constant input admittance as a function of frequency. Total power transfer occurs at zero frequency, and half-power transfer occurs at an input angular frequency of one radian per second. The prototype network is converted to a network having total power transfer at some frequency ω_0 through use of the angular frequency mapping function

$$\omega' = Q_L\left(\frac{\omega}{\omega_0} - \frac{\omega_0}{\omega}\right), \tag{1}$$

where

ω' = angular frequency variable of the prototype network
ω = angular frequency variable of the desired network
Q_L = $\omega_0/(\omega_1 - \omega_2)$
ω_1, ω_2 = half power angular frequencies of the desired network.

For the purpose of obtaining a qualitative understanding of electrical behavior it is sufficient to state that the performance of the microwave structure will be identical to that of the frequency-mapped prototype network subject only to the approximations involved in relating their respective parameters.

Four filters were constructed for use in the repeater system. The results were consistent from filter to filter. Figs. 9 and 10 show a set of typical characteristics. The insertion loss to the dropped channel is about 0.5 dB. The theory predicted an overall bandwidth of 1.13 GHz. The agreement between measured and theoretical values is good.

3.4 *Solid-State Millimeter-Wave Power Sources*

Three different solid-state millimeter-wave power sources were used. They were an LSA diode oscillator, an harmonic generator and an IMPATT diode oscillator.

The first solid-state device used successfully in the repeater was an LSA oscillator.[8] The diode used in this experiment required dc power of 0.4 amps at 3.5 volts and delivered 4 mW of power at 50.4 GHz. (Similar units which deliver 20 mW at various frequencies in the 40- to 100-GHz band have been built by Copeland.) The LSA oscillator was used in all of the error-rate and gain experiments described in Section V.

The varactor quadrupler uses a zinc diffused gallium arsenide diode.[15] The diode was a planar array structure similar to the "honeycomb"

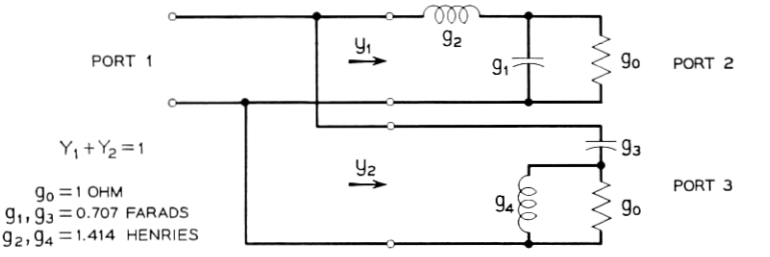

Fig. 8 — Prototype network for a two-pole diplexer.

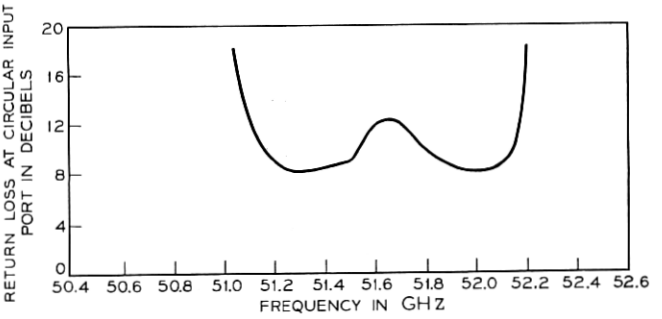

Fig. 9 — Return loss at port 1.

type described by Young and Irvin.[16] It was mounted in a Sharpless wafer as shown in Fig. 11. The input signal frequency was 12.6 GHz. The power output and overall efficiency of a typical unit are shown in Fig. 12. The maximum power output obtained was 10 mW at an efficiency of 6.5 percent. The input VSWR was less than 2 to 1 and the output VSWR was about 7 to 1. The power source for the quadrupler was an IMPATT oscillator which provided a 12.6-GHz signal.

The millimeter-wave IMPATT diode delivers approximately 50 mW at 50.4 GHz. (Diodes of this type which deliver 130 mW at 70 GHz have been built by T. Misawa.[17])

Each of these power sources gave an overall performance as good as that obtained from an Oki Klystron.

3.5 *Local Oscillator (LO) Injection Filters*

The local oscillator power is coupled to the up- and down-converters by means of a three port diplexer as shown in Fig. 13. The local oscil-

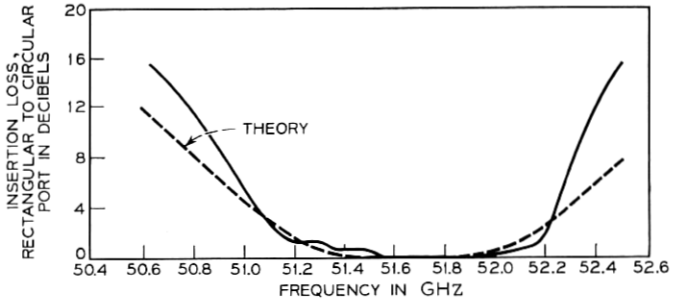

Fig. 10 — Insertion loss from port 1 to port 2.

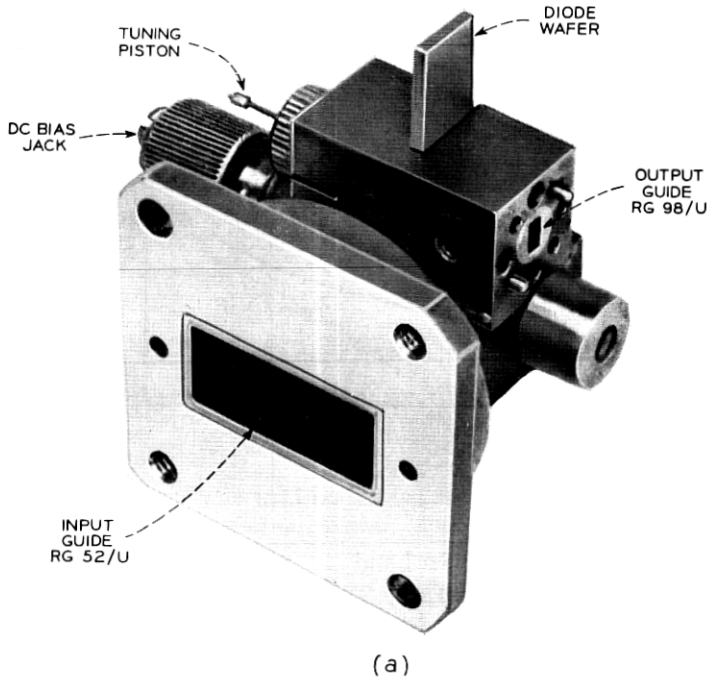

Fig. 11 — The X-band to millimeter-wave band quadrupler. (a) Photograph. (b) Cross-section view.

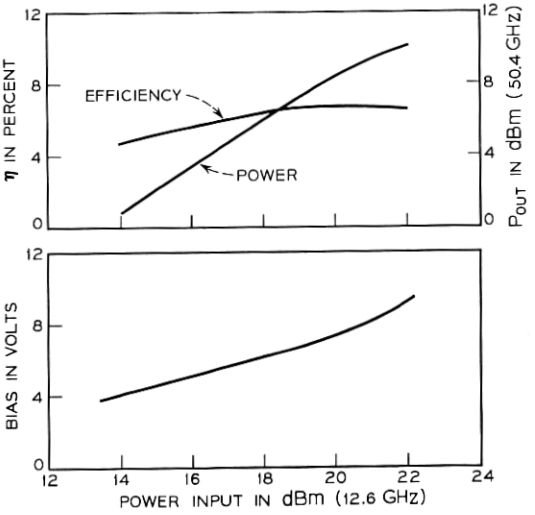

Fig. 12 — Power output and efficiency of quadrupler.

lator power is injected at the bandpass port (port 1) and the signal at the band rejection port (port 3). The up (or down) converter is connected to the constant resistance port (port 2).

The construction of an efficient millimeter wave diplexer was accomplished by utilizing two low-loss TE_{011} circular cylindrical cavity mode resonators as shown in Fig. 14. The device operates as follows. Both resonators are tuned to the local oscillator frequency. At resonance, the rejection cavity effectively open circuits the waveguide. The bandpass resonator (dropping filter) is located an odd number of quarter wavelengths from the transverse symmetry plane of the rejection resonator. Hence, at resonance, a short circuit appears to exist at plane A of Fig. 14.

Ideally, proper adjustment of the coupling apertures yields coupling

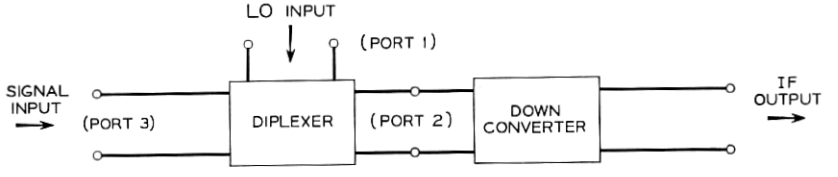

Fig. 13 — Schematic of the local oscillator injection arrangement.

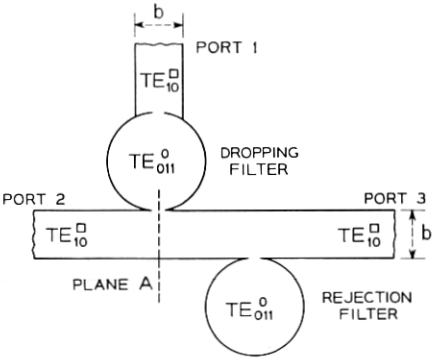

Fig. 14 — Physical realization of local oscillator injector filter.

of 100 percent of the LO power to port 1 in the absence of dissipation. The details of the design procedure are given in Ref. 18.

The requirements on the bandwidth of the diplexer were established by considering the tolerable dissipation of LO power at resonance, and the transmission loss through the diplexer over the signal band. The tolerable LO loss was set at 2 dB maximum based on the millimeter-wave power available from the solid-state source and the LO power requirements established for the up- and down-converters. Minimum attenuation to the signal band is achieved when the bandwidth is at a minimum consistent with the LO loss requirement. Experimental work indicated that a 50-MHz bandwidth in the power transfer from the LO input port to the converter port was about optimum.

Four diplexers were constructed with consistent results. The insertion loss to the LO averaged 1.4 dB. The return loss at the signal input port was better than 25 dB over the signal band. The return loss looking into the converter port was better than 15 dB at all frequencies of interest. Figs. 15 and 16 show typical frequency responses at the various ports.

3.6 *Down-Converters*

The down-converters developed for the system had the following characteristics:

(*i*) IF frequency band from 1.0 to 1.6 GHz
(*ii*) LO frequency of 50.4 GHz at a power level of −3 dBm
(*iii*) Input signal from 51.4 to 52.0 GHz
(*iv*) Conversion loss of 6.0 ± 0.5 dB over the above band
(*v*) Converter noise temperature ratio of nearly unity.

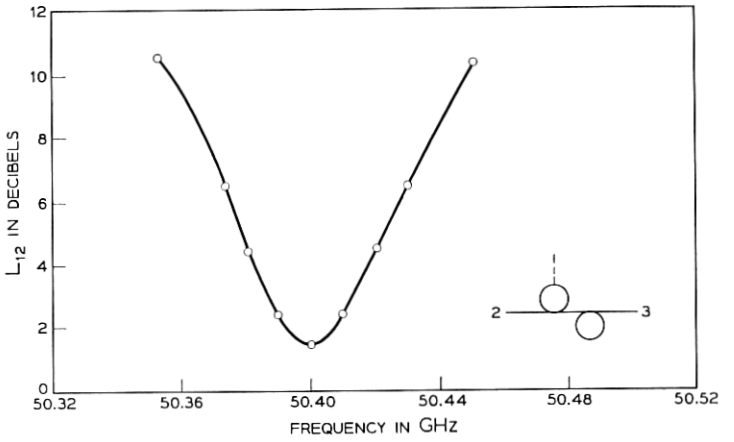

Fig. 15 — Pass-band response for local oscillator injection filter (ports 1 to 2).

This performance was achieved using Schottky barrier diodes at a fixed dc bias.

The basis for the design was the converter mount described by Sharpless.[19] The only modification required was the addition of an IF impedance matching network. The millimeter-wave portion of the structure was not changed. Fig. 17 shows the structure. The following paragraphs describe the equivalent circuit and give a brief discussion of the design procedure.

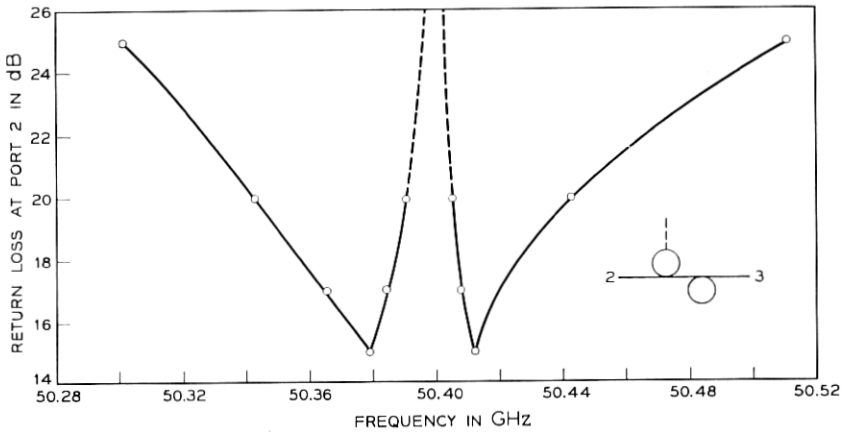

Fig. 16 — Return loss of local oscillator injection filter at port 2.

The equivalent circuit for the structure is shown in Fig. 18. The IF input admittance Y_L was measured over the band with the LO on and the bias fixed. It was found that Y_L could be closely approximated by a constant conductance shunted by a capacitive susceptance. At mid-band

$$Y_L = (59)^{-1} + j(150)^{-1} \text{ mhos.}$$

The admittance Y_L was matched to 50 ohms at mid-band by a short length of transmission line having a characteristic impedance of 83 ohms. This was followed by a biasing tap consisting of a quarter wavelength 50-ohm stub by-passed to ground. The excellent broadband behavior of the completed circuit is indicated by the small variation of conversion loss over the band. The latter is shown in Fig. 19.

3.7 *IF Amplifiers*

Wideband transistor amplifiers (with a center frequency of 1.3 GHz) of the balanced integrated circuit type originally developed by Engel-

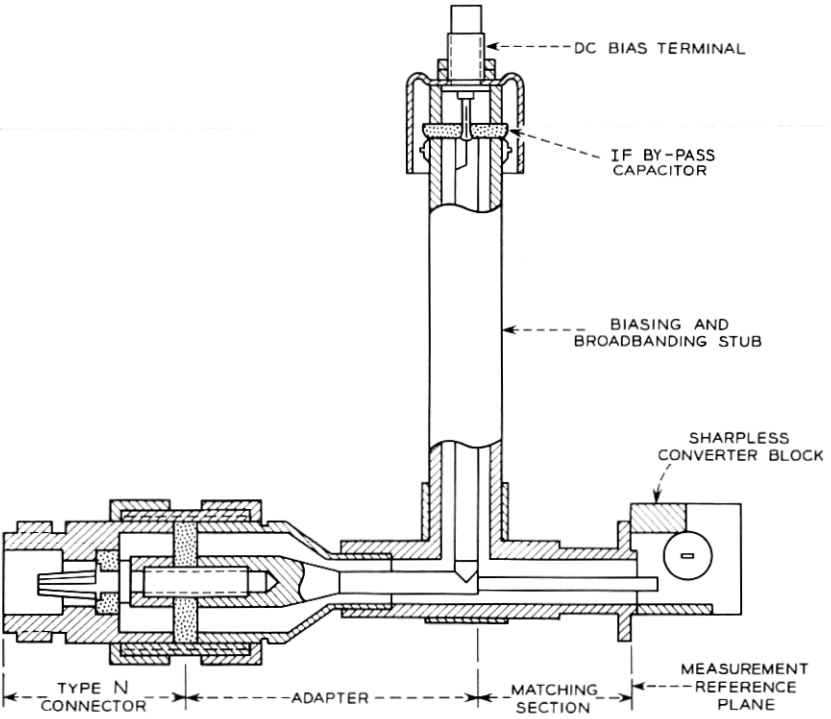

Fig. 17 — Down-converter structure.

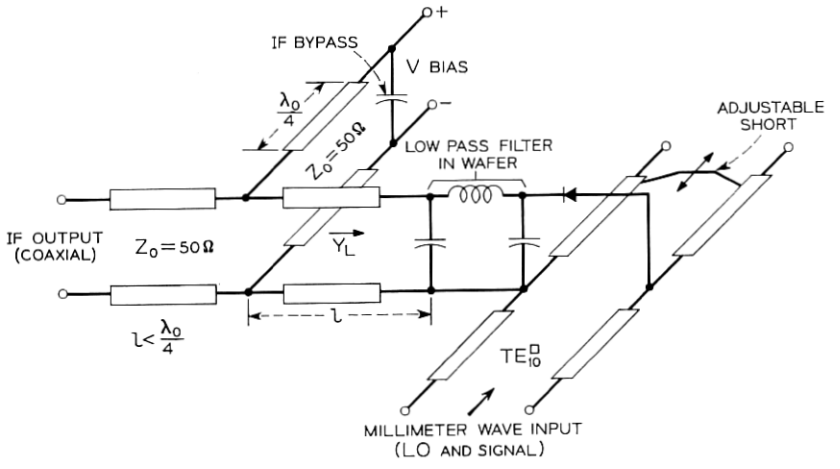

Fig. 18 — Down-converter equivalent circuit.

brecht and Kurokawa[20] were used in this repeater. Fig. 20, which is reproduced here from Ref. 20, shows the basic amplifier circuit. These amplifiers can be built with excellent noise figures (less than 4 dB) and, because of the excellent match between sections, can be cascaded to achieve high gain. These amplifiers exceeded the required specifications in all respects and have proved entirely satisfactory for this repeater.

3.8 *Limiter*

Because of the nature of the regenerator which is used in this repeater, an improvement in error-rate performance for a given signal-to-noise ratio is expected from the inclusion of a limiter ahead of the differential-phase detector.[21] A simple but effective limiter was

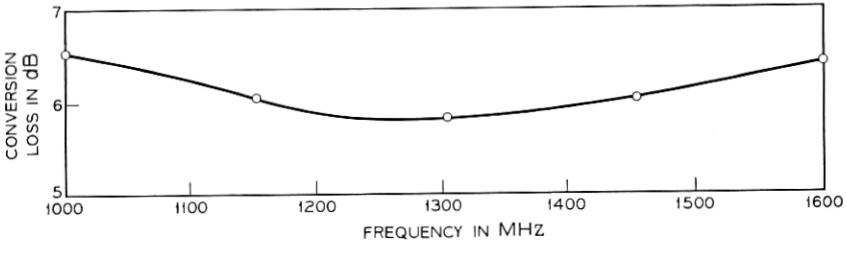

Fig. 19 — Conversion loss of down-converter.

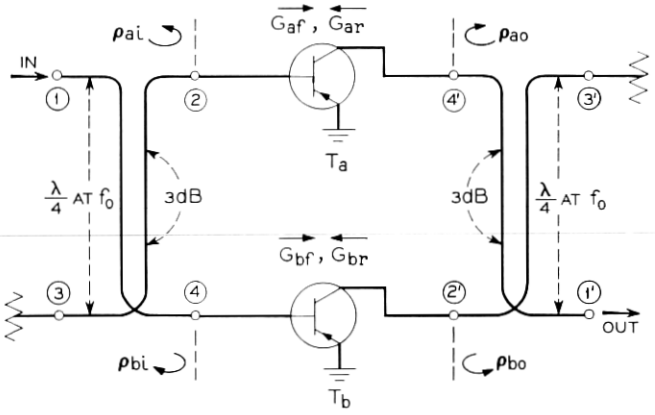

Fig. 20 — Schematic representation of single-stage balanced amplifier. (Taken from Ref. 20).

achieved by the use of a tunnel-diode oscillator built in 50-ohm coaxial transmission line and phase-locked to the IF signal (see Fig. 21). The tuning of the diode was inductive and was accomplished by means of a shorted 75-ohm transmission line stub. The tunnel diode was of germanium point-contact construction and had a peak current of 2 mA. Fig. 22 shows the output power of the oscillator versus gain (ratio of output power to input power) at the center frequency of the oscillator. Best error performance was found experimentally to occur at a gain of 8 dB. The change in output power with frequency for several values of gain is shown in Fig. 23.

3.9 *Differential Phase Detector and Timing Recovery*

The baseband and timing circuits are shown in Fig. 24. The couplers, delay lines, and diode mounts are microwave printed circuits; the filters and combining Tee are coaxial. The differential phase detector and the timing recovery circuit are combined (share a common delay line) in order to save space and cost.

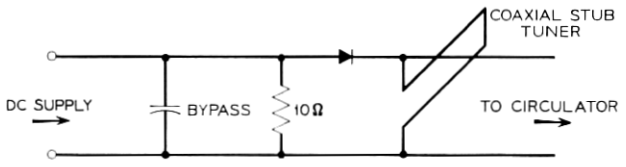

Fig. 21 — Limiter circuit.

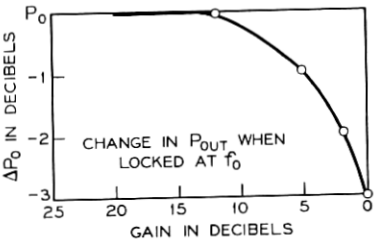

Fig. 22 — Output power of limiter vs gain at the center frequency.

Fig. 25 shows the basic differential-phase detector or timing-recovery circuit. A straightforward analysis (see the Appendix of Ref. 22) shows that the output voltage of this circuit is given by

$$V(t) = \cos\left\{\omega_0\tau + \int_{t-\tau}^{t} \omega(t')\,dt'\right\} \tag{2}$$

for an input FM-DCPSK signal given by

$$S(t) = \sqrt{2}\cos\left\{\omega_0 t + \int_{0}^{t} \omega(t')\,dt'\right\}, \tag{3}$$

with

$$|\,\omega(t)\,| = |\,\omega(t + nT)\,|, \qquad \int_{(n-\frac{1}{2})T}^{(n+\frac{1}{2})T} \omega(t')\,dt' = \pm\pi/2.$$

One can readily see that if $\omega_0\tau$ is chosen to be a multiple of π, $V(t)$ is independent, to first order, of the sign of $\omega(t)$; hence, the output is periodic in period T, where T is the reciprocal of the bit rate. By proper choice of $\omega_0\tau$ a signal is obtained with a strong frequency component

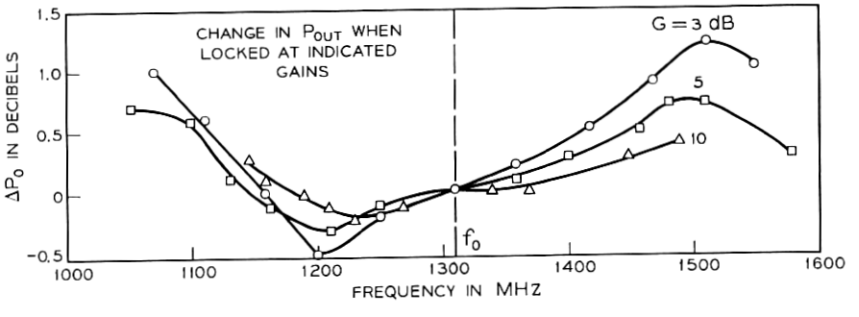

Fig. 23 — Change in output of the limiter vs frequency for several values of gain.

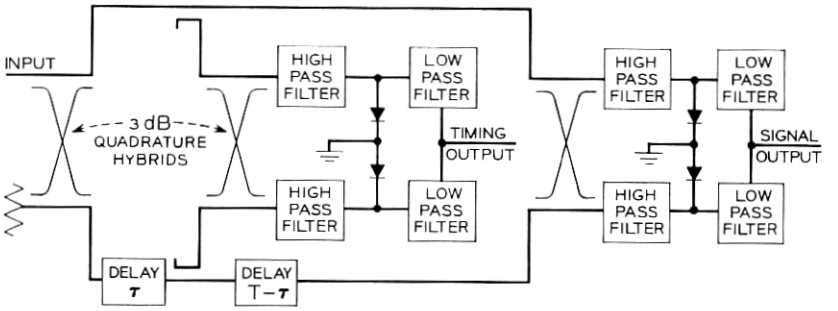

Fig. 24 — Differential phase detector and timing recovery circuit.

at the bit rate. This signal is used to lock an oscillator at the bit rate. The oscillator, in turn, provides the timing signal to the regenerator.

If $\omega_0\tau$ is chosen to be an odd multiple of $\pi/2$ and τ is chosen equal to T, the reciprocal of the bit rate, one sees from (2) and (3) that at the sampling instants, $[t = (n+\frac{1}{2})T]$, the output is given by

$$V(t) = \cos\{(m + \tfrac{1}{2})\pi \pm \pi/2\} = \pm 1.$$

Thus, under these conditions the device is the desired differential-phase detector for this signal.

3.10 *Regenerator*

The regenerator consists of a balanced-line logic element[23] which is a modification of the standard Goto-pair circuit. The input signal is applied at the midpoint between the two tunnel diodes and a timing signal is applied across the pair of tunnel diodes as shown in Fig. 26. Ideally, the timing signal causes one and only one of the diodes to switch once each time-slot. The input signal determines which of the two diodes switches. When one of the diodes switches, the resultant voltage drop across the other diode inhibits its switching and this voltage drop occurs across the output of the re-

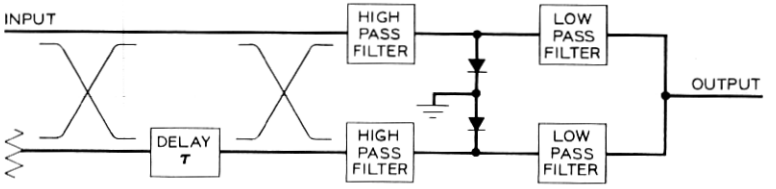

Fig. 25 — Basic differential phase detector or timing recovery circuit.

generator. If the diode labeled D_1 in Fig. 26 switches, the voltage pulse at the output of the regenerator is negative and, correspondingly, if D_2 switches the voltage pulse is positive. The transients initiated by the switching of the diode travel down the delay lines and are reflected with inverted polarity back to the diodes by the low-impedance termination. These reflected signals reset the diode to its original condition. Thus, the information content of the signal is translated into a sequence of polar baseband pulses at the regenerator.

E. G. Herzog[24] has discussed limitations on the speed of operation of the Goto-pair. His conclusions also apply to the balanced-line logic element. He showed that for bias voltages above a certain critical value the Goto-pair has a stable zero output state in addition to stable positive and negative output states. Due to the junction capacitance and the series inductance of the diode, it takes a finite time (talking time) for one diode to indicate to the other that it has switched. Thus, with a small input signal each diode can go to its second positive resistance region and if the synchronizing voltage passes the critical value too soon they will be left there and the zero output state will result. Also, we have observed that if the voltage does not pass the critical values soon enough both diodes will return to their first positive resistance region resulting in an intermediate amplitude output. In order to minimize the probability of occurrence of these undesirable operations, the following properties are desirable for the diodes: First, the diode must have adequate peak current (if the peak current is too

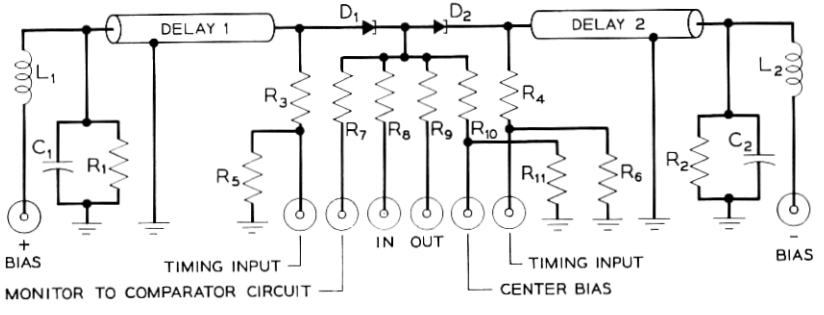

Fig. 26 — Regenerator circuit.

low, the load will prevent bistable operation); second, it must have low junction capacitance (this decreases the talking time); third, the magnitude of the product of the negative resistance and the junction capacitance should be low enough to make the switching time short compared with a time-slot; and finally, the diode should have low series inductance (this decreases the talking time). For the regenerator, the third condition must be strengthened to make the switching time short compared to the round-trip time on the delay line. Since several round trips are required for the pulse to die out, the switching time of the diodes in the balanced-line logic element must be several times faster than for a Goto-pair.

TD-252A germanium tunnel diodes have been found to meet the above requirements. They have a series inductance of 1.5 nH, a peak current of 4.7 mA and a junction capacitance less than 1.0 pF. The diodes are mounted in the circuit of Fig. 26 in the manner shown in Fig. 27. This circuit has been built in such a way that the diodes are placed as close together as possible in order to eliminate lead inductance. By building the diodes into the transmission line, connector mismatches have been eliminated. The inductance of the leads of the input and output resistors has very little effect on the output pulse and it is believed that it steers the current from one diode to the other during the short time required for switching. Fig. 28(a) shows an eye diagram of a low signal-to-noise ratio input signal to the regenerator and Fig. 28(b) the resulting output signal of the regenerator. This figure illustrates the ability of the regenerator to remove noise from the signal.

3.11 *FM Deviator*

The FM deviator is basically a tunnel-diode relaxation oscillator. The frequency of oscillation of the tunnel diode in this type of circuit is extremely sensitive to bias voltage, allowing it to be driven by the balanced-line logic element. Fig. 29 shows the circuit. Tests on a low-frequency prototype circuit showed that the oscillator could be tuned over a bandwidth of more than half an octave in a time interval corresponding to less than 1 RF cycle. The total tuning range of the *L*-band deviator was greater than an octave, as shown in Fig. 30.

The circuit of Fig. 29 was built for use in L-band using conventional (as opposed to printed) circuits with the circuit dimensions kept as small as possible. Fig. 28(c) shows the differentially detected output eye of the deviator.

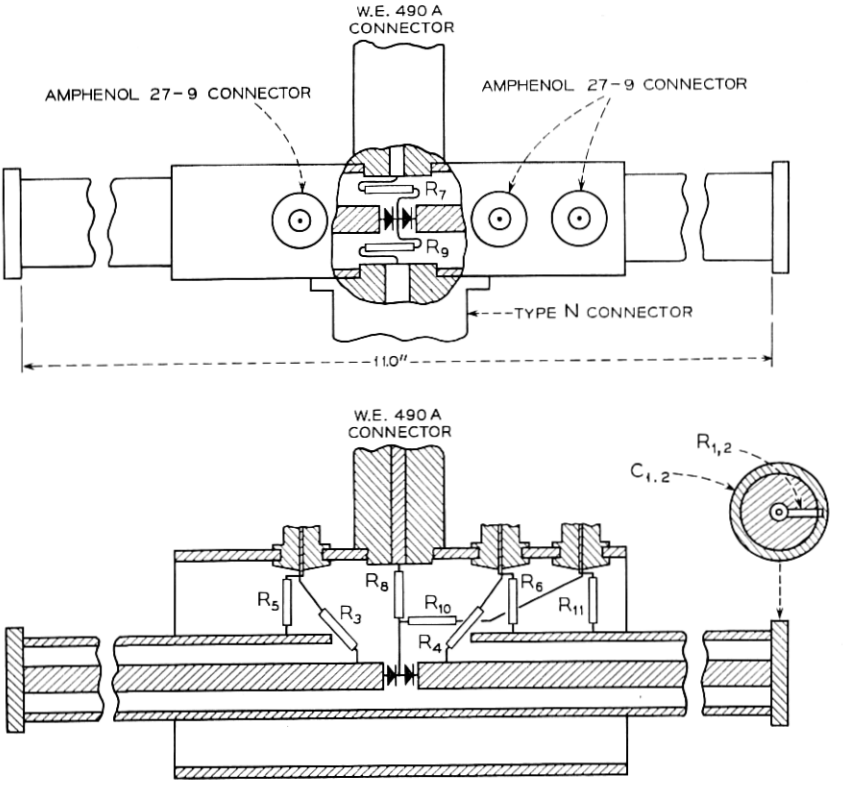

Fig. 27 — Mechanical layout of the regenerator.

3.12 *Up-Converters*

The chief goal in designing the up-converters was the maximization of output power over the band from 51.4 to 52.0 GHz when used with a local oscillator supplying + 3 dBm of power at 50.4 GHz. Typical units exhibited 6-dB LO to RF conversion loss across the band. Fig. 31 shows the frequency response of a typical unit. Both GaAs Schottky barrier diodes and planar diffused gallium arsenide varactor diodes were used with similar results—the latter exhibiting slightly lower conversion loss.

The physical structure for the units was similar in form to that of the down-converter described in Section 3.6. An *E-H* tuner preceded the converter block on the millimeter-wave side and was used to match the input impedance at the LO and signal band frequencies. All of the

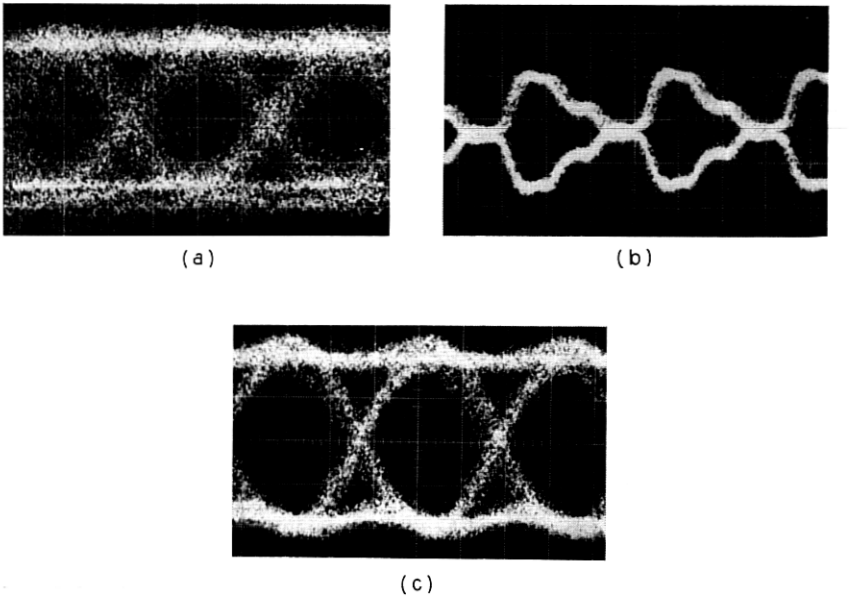

Fig. 28 — Eye diagrams. (a) Degraded regenerator input. (b) Regenerator output. (c) Regenerated differentially detected IF.

diodes were operated at zero bias voltage. A more detailed description of planar diffused diode performance is given in Ref. 15.

3.13 *Power and Space Requirements*

The baseband circuitry of the repeater requires approximately 0.3 watts and the IF circuitry requires approximately 1.5 watts. Thus, the power requirement per channel per repeater is approximately 1.8 watts exclusive of the power required for the millimeter-wave power source.

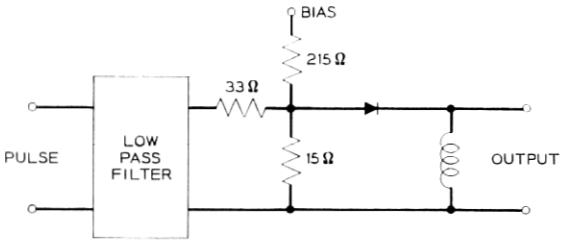

Fig. 29 — Deviator circuit.

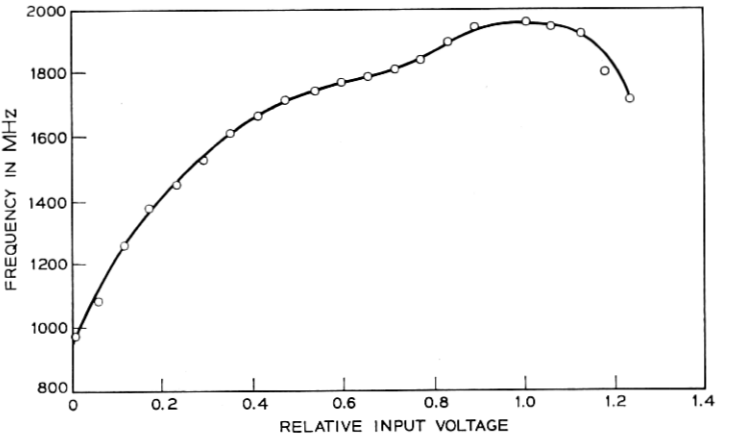

Fig. 30 — Deviator frequency vs relative input voltage.

The total power required per channel per repeater can thus be expressed by

$$\text{Total Power Required} = 1.8 + \frac{\text{Millimeter-Wave Power Required}}{\text{Efficiency of Millimeter-Wave Source}} \text{ Watts}$$

The experimental repeater included many commercial components and no serious thought was given to miniaturization. Even so, it occupies only a volume of the order of 2 cubic feet (exclusive of band-splitting filters). With printed circuit techniques, the total volume per channel per repeater can be of the order of 0.5 cubic feet or less.

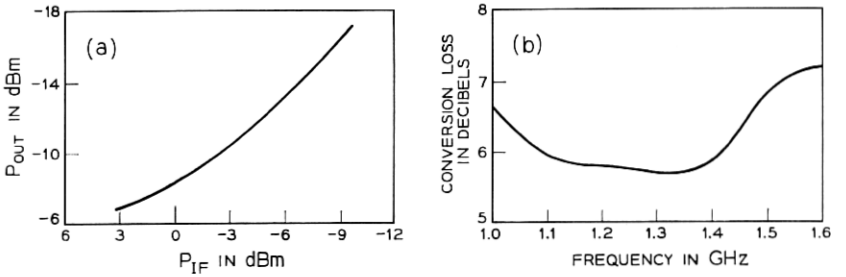

Fig. 31 — Varistor up-converter data. (a) Output versus input data. (b) Frequency response ($P_{IF} = +6$ dBm).

IV. SYSTEM CONSIDERATIONS

4.1 *Error-Rate as a Function of Signal-to-Noise Ratio*

The error-rate versus signal-to-noise ratio has been calculated in a manner which includes the effects of non-ideal regeneration of the signal and of intersymbol interference.[22] Some results of this calculation are shown in Fig. 32 for an ideal regenerator and for a regenerator which has a threshold of operation, T, 9 dB below the expected signal level, S. The term threshold of operation is defined as follows. Suppose that the expected value of the signal at the input to the regenerator is V_1 or $-V_1$. The regenerator will then regenerate a positive or negative output pulse according to whether the input is positive or negative. However, if magnitude of the signal is too small the regenerator will not function properly. The minimum voltage at which the regenerator will function properly is the threshold of operation.

It is impossible to consider quantitatively the effects of intersymbol interference unless the waveform of the signal is known accurately. However, it is plausible to assume that the intersymbol interference contributes phase shifts of the order of a few degrees in the sense described in Ref. 22. For that reason, Fig. 32 shows the results of error-rate versus signal-to-noise ratio for the case where there is no inter-

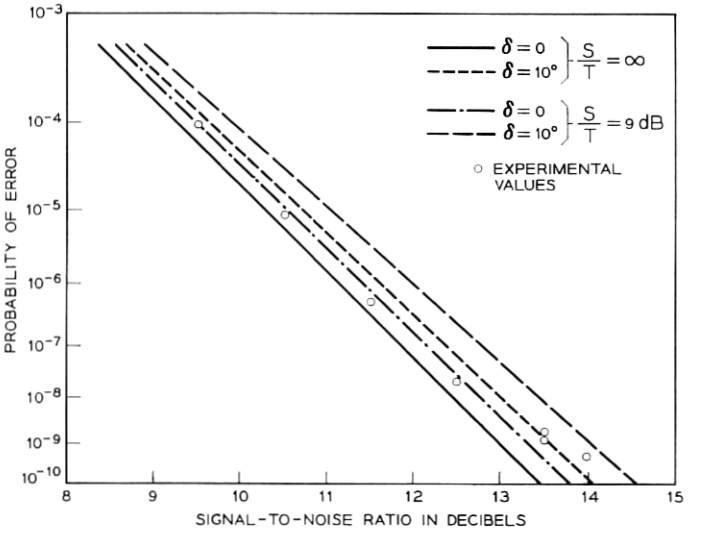

Fig. 32 — Error-rate vs Signal-to-noise ratio for the repeater.

symbol interference and for the case where the intersymbol interference corresponds to a phase shift, δ, of 10 degrees. These values should constitute the bounds on the expected error-rate. From Fig. 32 one observes that the expected value of S/N for 10^{-9} error rate lies between 13 and 14 dB.

4.2 *Model of a System*

Fig. 33 shows a model of a system which was used as an aid in the design of the repeater. This model is not an attempt to describe or design a complete system, it is intended only to give some perspective and insight into those factors which influenced the design of the repeater.

An actual system would use both frequency division and time division multiplex to separate individual voice channels. One possible arrangement of filters to separate the individual frequency multiplexed channels in the system is shown in Fig. 34. The skew arrangement of the filters is chosen to offset in part the variation of loss with frequency in the waveguide bandwidth. That is, since certain channels experience greater loss in the medium, the filters are arranged so as to give less loss to these channels at the expense of channels which have suffered less loss in the medium. Since the shape of the loss-versus-frequency curve is a function of repeater spacing (the relative loss in dB at two frequencies depends on the repeater spacing), the *details* of the arrangement of the filters are a function of repeater spacing. As an illustrative example, we assume a repeater spacing of 15 miles and attenuation curves for the medium given by Fig. 1. In addition, we

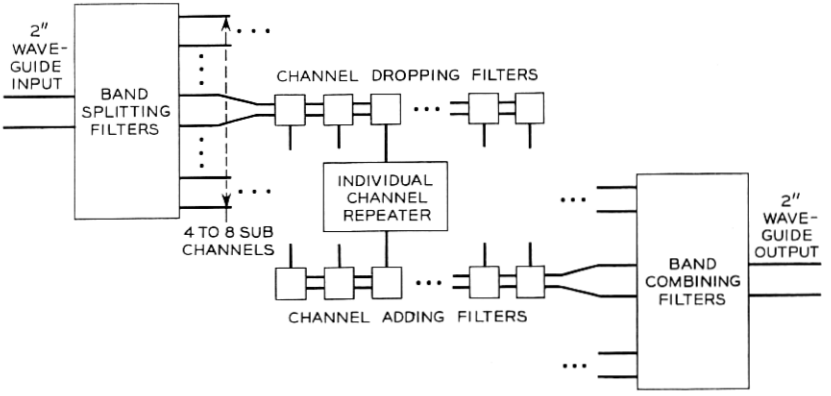

Fig. 33 — Illustrative model of a system.

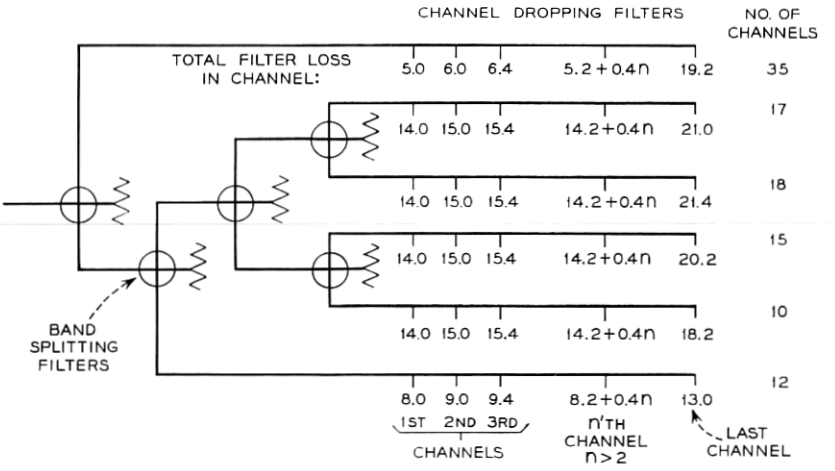

Fig. 34 — Channel-dropping filter array for the illustrative example.

make the assumption that the power available from realizable solid-state sources falls off at a rate of 3 dB per octave in frequency.[25] The loss of each band-splitting filter is taken to be 1.5 db.[12] Based on the data of Figs. 9 and 10, conservative estimates of channel-dropping filter losses are 1.0 dB to the dropped channel, 0.5 dB to the adjacent channel and 0.2 dB to all other channels which pass through them.

Fig. 35 shows the waveguide loss as a function of frequency for a 15 mile repeater spacing. It also shows the power at the input to a repeater relative to the power at the output of the up-converter of the 50-GHz channel (based on the curve of Nutt in Fig. 1 and the assumed 3 dB per octave fall off in available power). The points in the figure then show the total relative signal power at the output of the channel-dropping filter for each channel (based on the filter arrangement shown in Fig. 34). The term "relative power" here means the power relative to that available at the output of the up-converter in a 50-GHz channel. From Fig. 35 one observes that in the worst case the relative signal level is −58 dB for this model. Thus, the repeater gain (defined as the ratio of the output power of the up-converter to the signal power at the input to the down-converter which gives an error rate of 10^{-9}) must be 58 dB. Since this is the value which gives the *maximum acceptable* error-rate, it seems expedient to include a 6-dB margin in the design of the repeater and thus the design goal for a 15-mile repeater spacing is a gain of 64 dB.

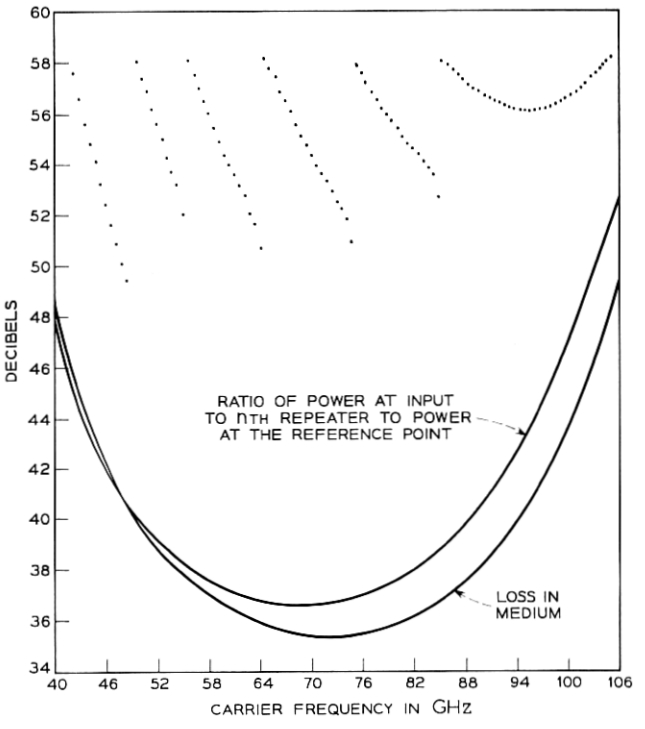

Fig. 35 — Ratio of power at the output of the channel-dropping filters to power at reference point. The power reference point is the output of the up-converter of the 50-GHz channel of the preceding repeater.

In this model, there are 100 channels spaced at 600-MHz intervals across the band. The experimental repeater described here uses a 500-MHz bandwidth set by an inexpensive commercially available five-section Tschebycheff filter. (Only a slight degradation is experienced by using a 400-MHz filter of the same type.) Even smaller bandwidths might well be practical if suitable attention is given to the phase characteristic of the filters. Thus, the 600-MHz spacing assumed in the model is a conservative estimate. The capacity of the waveguide based on this model is 30,000 Mb/s. Since 72 Kb/s are required for each voice-grade circuit, the capacity of the system would be 416,000 voice-grade circuits or 208,000 two-way voice channels.

4.3 *Theoretical Gain*

The gain of the repeater in the sense in which it is used here can be expressed as

$$G = (P_{LO} - L_{UC} - L_I) - (L_{DC} + F + KTB + \text{S/N}), \quad (4)$$

where

P_{LO} is the local oscillator power,
L_{UC} and L_{DC} are the conversion losses of the up- and down-converters, respectively,
L_I is the loss in the isolator, the waveguide between the LO and the up-converter, and the injection filter
F is the noise figure of the first IF amplifier (since one finds experimentally that aside from conversion loss, the noise figure of the down-converter is negligible),
KTB is the thermal noise in the pass band of the IF section, and
S/N is the signal-to-noise ratio required for the acceptable error-rate.

As stated in Sections 3.12 and 3.16, one finds experimentally that

$$L_{UC} = 6 \text{ dB}, \quad L_{DC} = 6 \text{ dB} \quad \text{and} \quad F = 3.7 \text{ dB}.$$

Using a 500-MHz bandwidth, the thermal noise power is -87 dBm. Therefore, the required local oscillator power for 15-mile repeater spacing is

$$P_{LO} = \text{S/N} + L_I - 7 \text{ dBm}.$$

If one assumes a value of 14 dB for S/N (from the discussion in Section 4.1) and 4 dB for L_I, he obtains 11 dBm as the required local oscillator power at the up-converter for a 15-mile repeater spacing. Since 0.5 mW of LO power is required for the down-converter, the total millimeter-wave power requirement for a 15-mile spacing is approximately 12 dBm.

V. EXPERIMENT AND RESULTS

5.1 *Description of the Apparatus*

The experimental apparatus used in the experiments to be described in Sections 5.2 and 5.3 consists of a transmitter, a receiver, and the repeater described in Section III as well as the necessary equipment and circuits for counting the errors made by the repeater, the receiver, or both. The transmitter is shown (in block diagram) in Fig. 36. The random-word generator consists of a regenerator of the type described in Section 3.10 driven by a similar regenerator which is, in turn, driven by differentially-detected wideband noise generated in a pair of X-band traveling-wave tubes. The random-word generator drives an FM deviator of the type described in Section 3.11. The remainder of

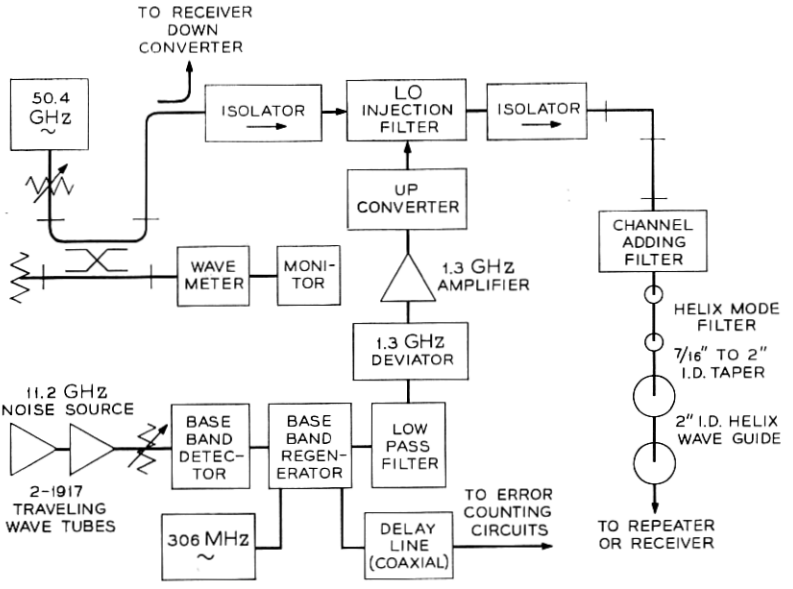

Fig. 36 — Transmitter.

the transmitter is identical to the portion of the repeater which follows the FM deviator.

Just as the transmitter is a duplicate of the second half of the repeater, the receiver is a duplicate of the first half, beginning with the down-converter and ending with the regenerator. It is shown in Fig. 37.

All of the regenerators (including the random-word generator of the transmitter) are built with two outputs—one to drive the next following component in the circuit, the other to serve as a monitor port or as a source of pulses for error counting. The three pieces of apparatus, the transmitter, the repeater and the receiver are built so that they can be interconnected in either of two ways; the transmitter can be connected to the repeater which is in turn connected to the receiver, or the transmitter can be connected directly to the receiver. This affords an *A-B* test of the performance of the repeater which is the heart of the gain experiment to be described in Section 5.3.

5.2 *Error-rate vs S/N Experiment*

One of the experiments performed with this apparatus measured the error-rate as a function of signal-to-noise ratio. This experiment

was performed for the four possible cases, namely, errors introduced by the transmitter to repeater hop, those introduced by the repeater to receiver hop, those introduced by the transmitter to receiver hop, and those introduced by the complete transmitter to repeater to receiver hops. Allowing for the differences in the noise figures of the actual devices used in each of these components, the results were quite consistent. Therefore, the experiment will be described for one case only, transmitter to repeater.

The signal from the extra output of the random word generator was delayed in a transmission line for a time interval equal to the time for the transmitted signal to be regenerated. The outputs from the random word generator and from the regenerator of the repeater were then combined in a "baseband hybrid" as shown in Fig. 38. The output of this "hybrid" is 0 if the two input pulses are of the same polarity and is some amount $\pm v$ if the input pulses differ in polarity indicating that an error was made. These output pulses drive a pulse-height discriminator which has two output channels. This device delivers a pulse to one of its two outputs if the magnitude of the input pulse exceeds a certain threshold value. If the input pulse is positive the output occurs in one channel; if the input is negative the output occurs in the other channel. These "error-pulses" are counted on a dual-channel counter.

The experimental procedure is quite similar to that used in performing similar experiments on a prototype model of the IF portion of this repeater. It is described in some detail in a previous paper[26] and need not be repeated here. Certain differences should, however, be pointed out. First, the error-counting technique has been improved by the use of the dual-channel counter as described above. Second, in this experiment the signal-to-noise ratio was adjusted by changing the signal level and using the actual amplifier noise instead of injecting additional noise into the input of the repeater as was done in the experiment of Ref. 26. Finally, in addition to the checks on signal statistics listed in Ref. 26, the IF signal was observed on a spectrum analyzer.

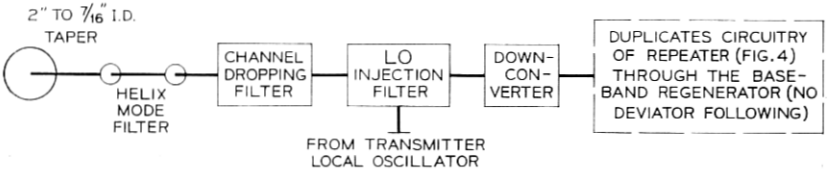

Fig. 37 — Receiver.

The biases on the random-word generator were adjusted until the spectrum was symmetric and free of "horns" or spikes (which are indicative of periodicities and hence nonrandomness in the signal).

The results of this experiment are shown by the points plotted in Fig. 32. Comparison between theory and experiment can readily be made from this figure.

5.3 *Repeater Gain Experiment*

The second experiment consisted of setting up two arrangements of components mentioned in Section 5.1 and setting the attenuators between these components to the value which gave an error rate of one error in 10^9 pulses (the assumed acceptable error-rate). This experiment is illustrated in block diagram form in Fig. 39. The gain of the repeater (in the sense of Section 4.3) is then given by

$$\text{(Loss from Trans. to Rep.)} + \text{(Loss from Rep. To Rec.)} - \text{(Loss from Trans. to Rec.)}$$

after allowance is made for loss in the passive millimeter-wave circuitry of the repeater. Experimentally, the loss between the transmitter and the receiver was found to be an amount A_0, the loss between transmitter and repeater plus the loss between repeater and receiver was found to be $A_0 + 43$ dB for 10^{-9} error probability at each regenerator. The loss in the passive millimeter-wave circuitry of the repeater was found to be 14 dB. Thus, the experimentally determined gain of the repeater is 57 dB. The measured local oscillator power is 6.0 dBm. From this one concludes that an additional 7 dB of LO power or a total of 13 dBm is necessary to achieve the 64-dB gain required for 15-mile repeater spacing with a 6-dB margin (from Section 4.2). This is in good agreement with the 12 dBm predicted by the argument of Section 4.3.

VI. CONCLUSIONS

A solid-state millimeter-wave repeater has been built which operates at a 306-Mb/s rate with an error-rate performance within 0.5 dB of

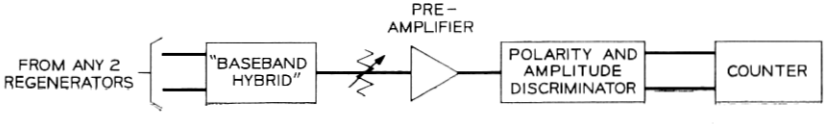

Fig. 38 — Error-counting circuitry.

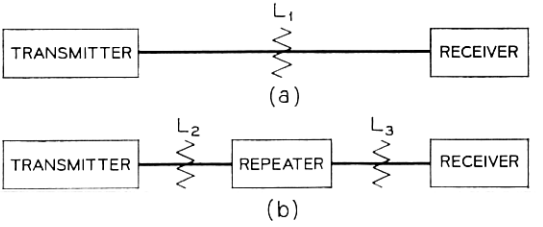

Fig. 39 — Experimental arrangement for gain test. L_1 = loss from transmitter to receiver, L_2 = loss from transmitter to repeater, L_3 = loss from repeater to receiver.

the theoretical value. It gives a measured gain of 57 dB with a local oscillator power of 6 dBm. Since the repeater gain is proportional to LO power it is concluded that a 13-dBm local oscillator would give the 64-dB gain necessary for a 15-mile repeater spacing with a 6-dB margin and a suitable channel-dropping filter array for over one hundred 300-Mb/s channels.

VII. ACKNOWLEDGMENTS

The authors are particularly grateful to Mr. R. S. Engelbrecht and Mr. J. A. Copeland for providing LSA diodes immediately upon their first successful operation, and to Mr. A. Bakanowski for supplying the IF amplifiers used in this experiment. We wish to thank Mr. C. A. Burrus and Mr. J. C. Irvin for providing the millimeter-wave diodes used in this experiment and Mr. B. C. DeLoach and Mr. T. Misawa for the *X*-band and millimeter-wave IMPATT diodes. We also thank Mr. C. N. Dunn for supplying the tunnel diodes for the limiters.

We wish to thank Mr. J. H. Johnson for developing the limiter and gratefully acknowledge his assistance in the construction of the IF and baseband circuits. We are grateful to Mr. H. M. James for constructing the clock and timing recovery circuits.

APPENDIX

A.1 *Introduction*

Several types of delay distortion equalizers have been proposed during the past several years. Five of these equalizers will be discussed in the following paragraphs. Any of the five could, in principle, be used to equalize the delay distortion of the waveguide; economic considerations will dictate which is the most practical. It might, for eco-

nomic reasons, be desirable to use more than one type of equalization. For example, frequency frogging (Paragraph A.3) might be used to give partial equalization with a transversal equalizer used to complete the equalization. Other possible combinations will suggest themselves as the advantages and disadvantages of each type of equalizer are discussed.

Delay distortion is inversely proportional to the cube of the frequency. The delay distortion introduced across a 500-MHz band by 15 miles of waveguide varies from 34 nsec at 40 GHz to 2.2 nsec at 100 GHz. Therefore, considerable equalization is necessary in the lower bands and some equalization is desirable (although not required) in the upper bands.

The pertinent characteristics of the delay distortion are summarized as follows. The time delay, T, in a length, l, of waveguide can be written as

$$T = \frac{l}{v_g} = l\frac{\partial\beta}{\partial\omega},$$

where v_g is the group velocity in the medium and β, the waveguide propagation constant, is given by

$$\beta = \frac{\omega}{c}\sqrt{1 - (\omega_c/\omega)^2}.$$

Expanding β in a Taylor's series about ω_0, the center angular frequency of the channel, gives

$$T = l[\beta_1 + 2\beta_2(\omega - \omega_0) + 3\beta_3(\omega - \omega_0)^2 + \cdots], \tag{5}$$

where β_1, β_2 $\cdots$ are the expansion coefficients of the Taylor's series for β.

For frequencies and bandwidths of interest the terms of order β_3 and higher are negligible for the 2-inch waveguide. Since the β_1 term is a constant time delay, the only source of distortion is the β_2 term.

A.2 *Reflection Equalizer*

The reflection equalizer, proposed by J. R. Pierce and W. S. Albersheim,[27] is illustrated in Fig. 40. Since the higher-frequency components of the signal penetrate deeper into the taper before being reflected than the lower frequency components, their round trip transit time is longer. By properly designing the shape of the taper the distortion of the guide can, in principle, be exactly equalized. Equalizers of

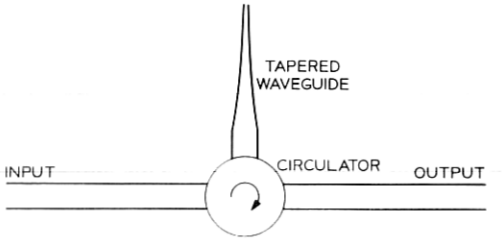

Fig. 40 — Reflection equalizer.

this type (operating at X-band) have been built by K. Woo[28] and also by C. C. H. Tang.[29] This type of equalizer can be built with an adjustable delay characteristic; as an alternative, one might build a small number of "stock" tapers which give approximate equalization and use a different type of equalizer to "trim" the equalization.

A.3 *Transmission Equalizer*

A second type of delay distortion equalizer is the transmission equalizer shown in Fig. 41. If the frequency spectrum of the signal in the channel is inverted and this signal is then passed through a short piece of waveguide near cutoff the delay distortion can be equalized since the frequency inversion causes a sign reversal in the β_2 term. Writing the transit time in the medium as

$$T_m = l_m[\beta_{1_m} + 2\beta_{2_m}(\omega - \omega_0)]$$

and the transit time in the equalizer as

$$T_e = l_e[\beta_{1_e} + 2\beta_{2_e}(\omega_0 - \omega) + 3\beta_{3_e}(\omega_0 - \omega)^2 + \cdots],$$

one obtains for the total transit time

$$T_m + T_e = [l_m\beta_{1_m} + l_e\beta_{1_e}] + 2[\beta_{2_m}l_m - \beta_{2_e}l_e](\omega - \omega_0) + 3\beta_{3_e}l_e(\omega_0 - \omega)^2 + \cdots .$$

The cutoff frequency of the equalizer can be chosen such that

$$\beta_{2_m}l_m = \beta_{2_e}l_e .$$

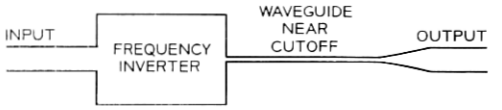

Fig. 41 — Transmission equalizer.

The delay distortion of the medium is thereby removed. If, however, l_e is short, the equalizer must be operated quite near cutoff in order to satisfy this equation. If l_e is too short, the terms of order β_{3e} and higher may contribute significant distortion to the signal. This, in fact, sets the lower limit on the length of the transmission equalizer. The minimum length of the equalizer depends on how much of this distortion is tolerable (which is not precisely known) and on the carrier frequency used in the equalizer. However, lengths of the order of ten feet or less are probably adequate for carrier frequencies above 50 GHz. For frequencies between 40 and 50 GHz, the length of the equalizer would probably be prohibitive for channel bandwidths of 500 MHz. However, transmission equalizers might be attractive as "trimming equalizers" for use with "stock" tapers or for use with the frequency-frogging scheme discussed in the next section.

Recently, J. H. Johnson[30] has built a transmission equalizer. His tests indicate that at the frequencies of interest, the phase characteristic is in agreement with the lossless theory and that the attenuation will not be prohibitive.

A.4 *Frequency Frogging*

The third approach to delay distortion equalization is due to D. H. Ring.[31] It is known as "frequency frogging" and consists of replacing every other regenerative repeater in the system with nonregenerative repeaters that invert the frequency spectrum of each channel and provide linear gain. This scheme is illustrated in Fig. 42. The medium itself in span 2 (see Fig. 42) then acts as a long transmission equalizer for span 1. If the spans are of equal length the equalization is exact except for the contribution from the β_3, β_5, etc., terms in (5) which is negligible for reasonable channel bandwidth and repeater spacings. If the spans are of unequal length, say x_1 and x_2, respectively, only the distortion $2\beta_2(\omega\text{-}\omega_0)(x_1\text{-}x_2)$ must be equalized. Since one would have

$$| 2\beta_2(\omega - \omega_0)(x_1 - x_2) | \ll | 2\beta_2(\omega - \omega_0)x_1 |$$

the "trimming equalizer" required in such a system could be a comparatively simple transmission or transversal equalizer.

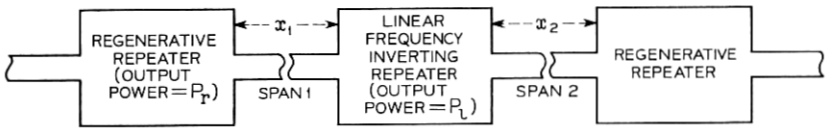

Fig. 42 — Frequency frogging.

The chief disadvantage of frequency frogging is the requirement that the nonregenerative repeater be linear.* This will probably result in lower available power at these repeaters than is attainable at the regenerative repeaters. The effect on repeater spacing can be calculated. If we define P_r and P_l to be the average power available at the output of regenerative and linear repeaters, respectively, x_0 to be the maximum allowable spacing between repeaters in a system having all regenerative repeaters and ideal delay distortion equalizers, and x_1 and x_2 to be the lengths of the spans in the frequency-frogging system, the values of x_1 and x_2 which maximize the quantity $x_1 + x_2$ are given by

$$x_1 = x_0 - 1 \text{ miles}$$

$$x_2 = x_0 - 1 - \frac{10}{3} \operatorname{Log} \frac{P_r}{P_l} \text{ miles.}$$

(A loss of 3 dB per mile has been assumed in the above equations.) The fractional decrease in repeaters spacing using this scheme is thus,

$$\frac{2x_0 - (x_1 + x_2)}{2x_0} = \frac{1 + \frac{5}{3} \operatorname{Log} \frac{P_r}{P_l}}{x_0} = \frac{1 + \frac{(P_r/P_l) \text{ dB}}{6}}{x_0}$$

which, for example, amounts to only about 12 percent for $P_r/P_l = 8$ dB and $x_0 = 20$ miles. The amount of delay distortion which must be made up by a "trimming equalizer" is equivalent to Δ miles of guide where

$$\Delta = x_1 - x_2 = \frac{10}{3} \operatorname{Log} \frac{P_r}{P_l}.$$

For the example cited above, $\Delta = 2.67$ miles.

A.5 *Transversal Equalizer*

Baseband transversal equalization can be used in a linear system to improve the pulse response.[32] This type of equalizer functions by adding time shifted images of the input pulse to itself in such a manner that the pulse response of the system is set to zero at a finite number of instants an integral number of time slots from the pulse center. The addition of the time shifted images of the pulse is usually carried out by means of a tapped delay line and a summing network.

* Since the delay distorted signal at the nonregenerative repeater may possess amplitude modulation, this repeater may have to be linear up to power levels higher than the average signal power.

Since the conversion to and from baseband in our system is nonlinear, baseband equalization cannot be used. However, an IF transversal equalizer can be used. A possible configuration of the circuit is shown in Fig. 43. It can be shown that any realizable transfer function can be approximated over a finite band using this type of circuit.[33] Thus, this circuit can be used to compensate for the waveguide delay distortion.

An alternate approach to transversal equalization can be used which is similar to baseband transversal equalization. It can be shown by taking quadrature components that the binary FM-DCPSK signal is equivalent to two polar pulse trains in phase quadrature. By proper choice of tap gains and phase shift the response of the system can be set to zero at instants that are multiples of a bit interval from the pulse center.

Computations made by one of the authors, JEG, which will be published at a later date, show that transversal equalizers with about 11 taps can be built to equalize the channels at 50 GHz and that above 70 GHz extremely good equalization can be achieved with 5 or fewer taps. Also, under certain circumstances, the phase shifters can be eliminated.

A.6 *Equalization by Quasi-Periodic Structures*

In a recent paper,[34] H. S. Hewitt has described a tapered meander line filter, shown in Fig. 44, which produced 300 ns of nearly linear delay distortion over a frequency band from 1.1 to 1.7 GHz. This device, which had a total length of less than 18 inches, demonstrates the feasibility of using a filter of this type. It is believed that this type of structure deserves careful consideration.

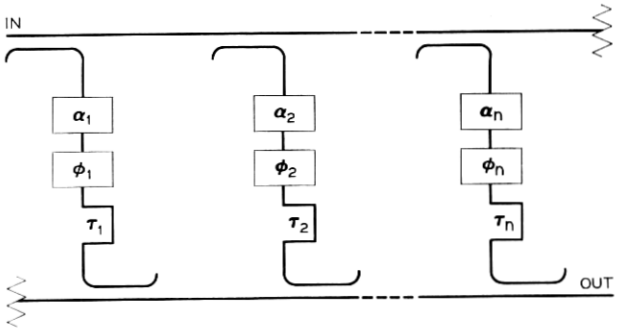

Fig. 43 — A microwave realization of the transversal equalizer.

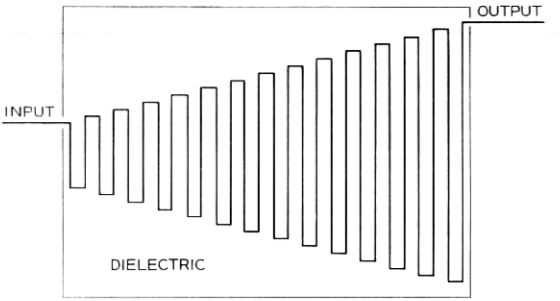

Fig. 44 — Tapered meander line.

REFERENCES

1. Miller, S. E., Waveguide as a Communication Medium, B.S.T.J., *33,* November, 1954, pp. 1209–1265.
2. Rowe, H. E. and Warters, W. D., Transmission in Multimode Waveguide with Random Imperfections, B.S.T.J., *41,* May, 1962, pp. 1031–1170.
3. Morgan, S. P. and Young, J. A., Helix Waveguide, B.S.T.J., *35,* November, 1956, pp. 1347–1384.
4. Unger, H. G., Round Waveguide with Lossy Lining, Proc. Symp. Millimeter Waves, Polytechnic Inst. of Brooklyn, 1959, pp. 535–541.
5. King, A. P. and Mandeville G. D., Observed 33 to 90 KMc Attenuation of Two-Inch Improved Waveguide, B.S.T.J., *40,* September, 1961, pp. 1323–1330.
6. Steier, W. H., The Attenuation of the Holmdel Helix Waveguide in the 100–125 KMc Band, B.S.T.J., *44,* May, 1965, pp. 899–906.
7. Nutt, W. G., private communication.
8. Copeland, J. A., CW Operation of LSA Oscillator Diodes— 44 to 88 GHz, B.S.T.J., *56,* January, 1967, pp. 284–287.
9. Kotel'nikov, V. A., *Theory of Optimum Noise Immunity,* McGraw-Hill Book Co. Inc., New York, 1959.
10. Lawton, J. G., Comparison of Binary Data Transmission, Proc. 1958 Conf. Mil. Elec.
11. Anderson, R. R. and Salz, J., Spectra of Digital FM, B.S.T.J., *44,* July 1965, pp. 1165–1190.
12. Marcatili, E. A. and Bisbee, D. A., Band Splitting Filter, B.S.T.J., *40,* January, 1961, pp. 197–212.
13. Standley, R. D., A Millimeter-Wave, Two-Pole, Circular-Electric Mode, Channel-Dropping Filter Structure, to be published, B.S.T.J., December, 1967.
14. Marcatili, E. A., Mode Conversion Filters, B.S.T.J. *40,* January, 1961, pp. 149–184.
15. Lee, T. P. and Burrus, C. A., A Millimeter-Wave Quadrupler and an Up-Converter Using Planar Diffused Gallium Arsenide Varactor Diodes; Conf. High Freq. Gen. Ampl., Cornell University, Ithaca, N. Y., August, 1967.
16. Young, D. T. and Irvin, J. C., Millimeter Frequency Conversion Using Au-n-Type GaAs Schottky Barrier Epitaxial Diodes with a Novel Contacting Technique, Proc. IEEE, *53,* December, 1965, pp. 2130–2131.
17. Misawa, T., CW Millimeter-Wave IMPATT Diodes with Nearly Abrupt Type Junctions, Solid-State Device Research Conf., Santa Barbara, Calif., June, 1967.
18. Standley, R. D., Millimeter Wavelength Diplexing Filters Utilizing Circular TE_{01} Mode Resonators, PGMTT, to be published, January, 1968.
19. Sharpless, W. M., Wafer-Type Millimeter Wave Rectifiers, B.S.T.J., *35,* November, 1956, pp. 1385–1420.

20. Engelbrecht, R. S., and Kurokawa, K., A. Wideband Low Noise L-Band Balanced Transistor Amplifier, Proc. IEEE, *53*, March, 1965, pp. 237–247.
21. Hubbard, W. M., The Effect of a Finite-Width Decision Threshold on Binary Differentially Coherent PSK Systems, B.S.T.J., *45*, February, 1966, pp. 307–320.
22. Hubbard, W. M., The Effect of Intersymbol Interference on Error-Rate in Binary Differentially Coherent Phase Shifted Keyed Systems, B.S.T.J., *46*, July–August, 1967, pp. 1149–1172.
23. Axelrod, M. S., Farber, A. S., and Rosenheim, D. E., Some New High Speed Tunnel-Diode Logic Circuits, IBM J., April, 1962.
24. Herzog, G. B., Tunnel-Diode Balanced-Pair Switching Analysis, RCA Rev., June, 1962.
25. Copeland, J. A., private communication.
26. Hubbard, W. M. and Mandeville, G. D., Experimental Verification of the Error-Rate Performance of Two Types of Regenerative Repeaters for Differentially Coherent Phase Shift Keyed Signals, B.S.T.J., *46*, July–August, 1967, pp. 1173–1202.
27. Pierce, J. R., Tapered Waveguide Delay Equalizer, U. S. Patent No. 2,863,126, issued December, 1958.
28. Woo, K., An Adjustable Microwave Delay Equalizer, IEEE Trans., *MTT 13*, March, 1965, pp. 224–232.
29. Tang, C. C. H., Delay Equalization by Tapered Cutoff Waveguides, IEEE Trans. Microwave Theory Tech., *MTT-12*, November, 1964, pp. 608–615.
30. Johnson, J. H., private communication.
31. Ring, D. H., U. S. Patent No. 2,629,782, issued.
32. Wheeler, H. A., The Interpretation of Amplitude and Phase Distortion in Terms of Paired Echoes, Proc. IRE, *27*, June, 1939, pp. 359–385.
33. Burrows, C. R., Discussion of H. A. Wheeler paper (see Ref. 32) pp. 384–385.
34. Hewitt, H. S., A Computer Designed, 720 to 1 Microwave Compression Filter, Group Microwave Tech. Int. Microwave Symp. Digest, 1967, pp. 51–53.